Novel liquid crystal display device for memory mode and dynamic mode

Jae Chang Kim, Chul Gyu Jhun, Chao Ping Chen, Seong Ryong Lee, and Tae-Hoon Yoon*
Dept. of Electronics Engineering, Pusan National University, Busan 609-735, Korea
Phone: +82-51-510-2375, E-mail: jckim@pusan.ac.kr

Abstract
So far, monostable and bistable LCD modes have independently been researched and developed. We introduce a novel liquid crystal display device that can be operated as memory mode as well as dynamic mode. This device has a unique texture of splay, π twist and bend states with applied voltages and is operated as a memory mode or dynamic mode by selective switching of two states among them. We also demonstrate electro-optical characteristics of the transmissive dual mode.

1. Introduction
Liquid crystal display (LCD) modes are basically classified into two categories, which are monostable and bistable modes. Monostable LCD modes have only one permissible state in the absence of external electric field. Many kinds of operating modes with monostable characteristics have been proposed for mobile display, monitor, and TV applications which require fast response time [1-7]. On the other hand, bistable modes have two stable states without applied voltage. The intrinsic memory characteristics of bistable modes are suitable for electronic book and electronic paper applications. A number of bistable modes have been proposed [8-14]. However, until now, monostable and bistable LCD modes have independently been researched and developed.

In this paper, we introduce a novel liquid crystal display device that can be operated as memory mode as well as dynamic mode, namely dual mode. The proposed device has a unique texture of splay, π twist and bend states with applied voltages and is operated as memory mode or dynamic mode by selective switching of two states respectively among the splay, π twist and bend states. This novel LCD device has not only a long term memory time for memory mode but also a fast response time for dynamic mode. We also demonstrate electro-optical characteristics of the transmissive dual mode.

2. Operating principle of dual mode
The textures of LCDs are determined by various factors such as liquid crystal parameters, alignment materials and conditions, pixel boundary conditions, etc. The display characteristics depend on the texture of LCDs as well. With the top and bottom substrates parallel rubbed and the addition of a chiral dopant of appropriate concentration in liquid crystal, we can obtain texture transitions of splay, π twist, and bend states by applying the appropriate electric field to each texture [8, 14-16].

Figure 1 shows the texture transition process from applying a corresponding electric field to each texture of the proposed device. When a vertical field is applied, the splay state (bottom left) is changed into a high bend state (top right) via a low bend state (top left). Then, if we remove the applied voltage, the bend state is relaxed into the π twist state (bottom right). Finally, when a horizontal field is applied, the π twist state returns back to the initial splay state [14-16].

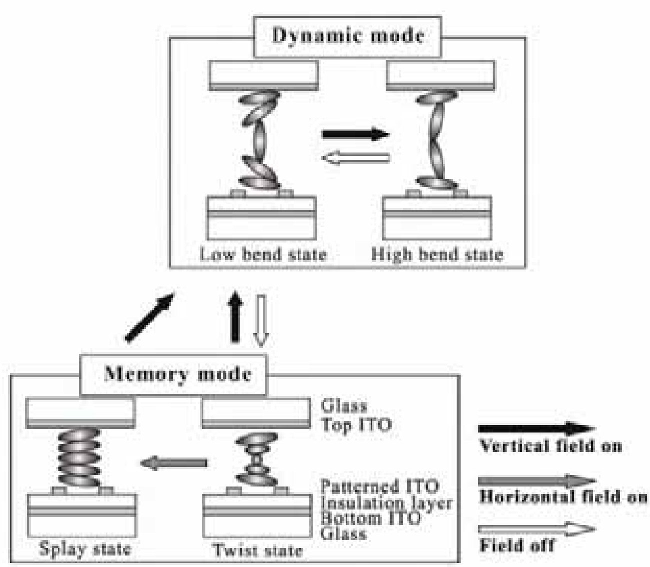

Figure 1. Transition process of dual mode.

This device exhibits bistable characteristics by blending a chiral dopant of appropriate concentration in the liquid crystal. Without external field, theoretically the free energies of the splay and π twist states are minimized and coincide at the d/p ratio of 0.25 [17, 18]. Topologically, the splay state is distinct from the π twist state. It was confirmed that π bistable twisted nematic (BTN) device using two topologically distinct states show longer memory time than 2π BTN device using two topologically equivalent states [13, 19]. Therefore, as memory states for a memory mode, splay and π twist states are more suitable. Although π twist state is more stable at the d/p ratio of 0.25, in our device, we chose a d/p ratio of 0.2, because the splay state should be more stable than the twist state for horizontal switching [14-16].

When a vertical electric field is applied to the device in the twist state, the twist state is switched to a bend state without the motion of disclination line due to the topological equivalence. As a consequence, the bend texture transited from the twist state is always relaxed into the twist state after removing the applied vertical field. Moreover, by applying an appropriate voltage, we can control the LC directors to be aligned in between the low and high bend states [16]. Therefore, we can obtain both bistable and monostable characteristics with the top and bottom substrates parallel rubbed and a d/p ratio of 0.2.

3. Optical design of dual mode

Figure 2 shows an optical configuration for the proposed dual mode. It is composed of two crossed polarizers, two compensation layers and a LC layer. The optic axes of the two compensation layers are parallel to each other and perpendicular to the rubbing direction of the LC layer. The angle between the optic axis of the compensation layer and the transmissive axis of the adjacent polarizer is 45°.

If the retardations of the LC layer and compensation layer are balanced out in a high bend state with an appropriate bias voltage, we can obtain a complete dark state over the whole visible spectrum for dynamic mode. On the other hand, for memory mode, the splay and twist states need to be optically distinguishable from each other. To optimize the retardation value of the memory mode, Jones matrix method was adopted for a simple approach [20]. The

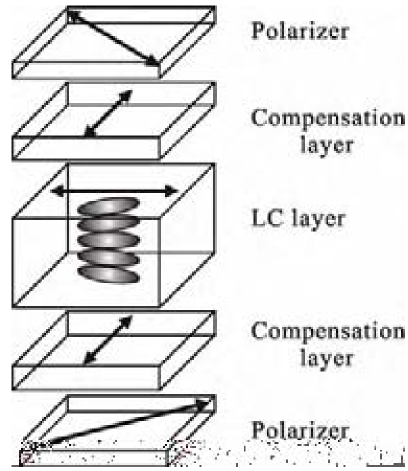

Figure 2. Optical configuration of transmissive dual mode.

transmittance is calculated from the polarization state of the emerging light. The Jones vector of the emerging light, E_{out}, after passing through the cell, is given by

$$E_{out} = P_{out} \bullet R(-\theta_{wp2}) \bullet W \bullet R(\theta_{wp2}) \bullet R(-\theta_{LC}) \bullet M_{LC} \bullet R(\theta_{LC}) \bullet R(-\theta_{wp1}) \bullet W \bullet R(\theta_{wp1}) \bullet E_{in} \;, \qquad (1)$$

where P, R, W, and M_{LC} represent the Jones matrix of the polarizer, coordinate rotation, compensation film, and LC layer, respectively [21-23]. After trivial calculations, we can obtain the transmittance of splay state as follows:

$$T_{splay} = (\sin(\delta - \gamma))^2, \qquad (2)$$

where

$$\delta = \frac{\pi}{\lambda} \Delta nd \qquad (3)$$

and γ is the total retardation value of the two compensation layers. The transmittance of the splay state depends on the retardation of LC layer and the compensation film. If the retardation of the LC layer is

$\delta = m\pi + \gamma$, where m = 0, 1, 2, 3…., (4)

the splay state exhibits a dark state.

In the case of a small retardation value of LC layer, the brightness is decreased because of twist configuration in the presence of chiral dopant [24]. Customarily, larger retardation of LC layer corresponds to higher brightness. However, the larger the retardation of the LC layer is, the worse the dispersion. Therefore, this novel LCD should be designed with an intermediate retardation value of LC layer, for instance m = 2.

We fabricated several test cells to investigate the electro-optical characteristics of the dual mode. A biaxial retardation film was used as the compensation layer. In-plane retardation (Ro) and out of plane retardation (Rth) of the compensation layer were 50 and 320 nm, respectively. An ITO coated glass and a three-terminal electrode structure were used. The substrates were coated with an alignment material, SE-3140 (Nissan Chemicals), which produced a pretilt angle of 5° after a rubbing process. The cell gap was maintained at 7.9 μm, which corresponds to in Eq. (4). A chiral additive material was doped in a liquid crystal, MLC-6204-000 (Merck), to yield a d/p of 0.2.

To measure the electro-optical characteristics of the fabricated tri-state LCD, a He-Ne laser of 543.5 nm wavelength was used as a light source. The transmitted light was measured using a PIN photodiode. The voltage waveforms applied to the test cell were generated using an arbitrary function generator. Both the applied voltage and the output of the photo-detector were simultaneously monitored on a digital storage oscilloscope. As shown in the voltage-transmittance curve of Fig. 3(a), a dark state was obtained at 5 V. At about 1 V, the twist to bend transition induced an optical bouncing. From the Fig. 3(b), the response time was measured with an applied voltage range between 2 and 5 V. The response time was 15.8 ms with the rising and falling times of 13.8 and 2 ms, respectively. The contrast ratio at normal direction was larger than 800.

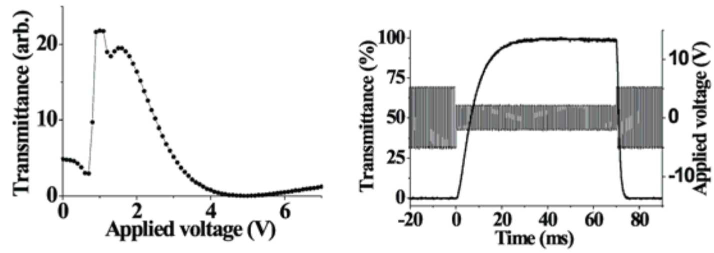

(a) (b)

Figure 3. (a) The measured V-T curve and (b) response time,

Figure 4 shows the electro-optical characteristics of the memory mode switching. As shown in Fig. 4(a), the splay to twist transition occurs upon application of a vertical voltage of 20 V for 500 ms. The twist state can return to the splay state upon application of a horizontal voltage of 40 V for 500 ms as shown in Fig. 4(b). The low and high transmittances represent the transmittances of the splay and twist states, respectively. The splay-to-twist and twist-to-splay transitions take 1.5 and 2 s, respectively. Permanent memory time was achieved in the splay state, because in our device, the splay state was the most stable state. On the other hand, the twist state was maintained for about 12 min, and the twist state was completely replaced by the splay state after 17 min. By forming a 90° twist domain around a pixel to prevent the motion of the disclination lines, we can obtain an infinite memory time of the twist state [25].

Each color of the two stable states is compared by the 1976 CIE color space [26]. The color is represented on the u*v* plane for a light source D_{65} as shown in Fig. 4 (c). By a spectrometer (MCPD-3000, OTSUKA ELECTRONICS), the chromaticity coordinates (L*, u*, v*) of the splay and twist states were measured as (59.151, 32.493, -43.701) and (67.967, -74.0187, 15.359), respectively. The color difference between the two memory states is 122.1088, which is calculated by

$$\Delta E_{uv}^{*} = [(\Delta L^{*})^2 + (\Delta u^{*})^2 + (\Delta v^{*})^2]^{\frac{1}{2}}, \quad (5)$$

where $\Delta L^{*} = L_2^{*} - L_1^{*}$, $\Delta u^{*} = u_2^{*} - u_1^{*}$, and $\Delta v^{*} = v_2^{*} - v_1^{*}$.

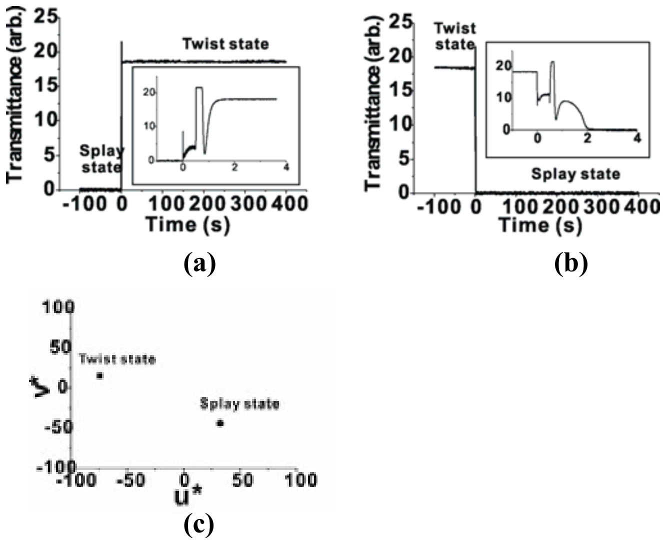

Figure 4. (a) Optical response for memory operating mode, and (b) Each color of two stable states is compared on the u*v* plane for the light source of D_{65} in the 1976 CIE (L*, u*, v*) chromatic coordinate.

3. Conclusion

We proposed a tri-state LCD mode which can be operated in both memory mode and dynamic mode, namely in dual mode. We confirmed the transition among splay, twist, and bend states by polarizing microscope and measured the electro-optical characteristics. For the dynamic operating mode, we obtained a high contrast ratio of more than 800 and a fast response time of 15.8 ㎳. The color difference was large enough to be used as a memory mode. We expect that the unique electro-optical characteristics of the tri-state LCD can open a fresh way to display applications by integrating the proposed memory and dynamic operating modes in a single device.

4. Acknowledgements

This research was supported by a grant (F0004052) from the Information Display R&D Center, one of the 21st Century Frontier R&D Program funded by the Ministry of Commerce Industry and Energy of the Korean Government.

5. References

[1] M. Schadt, and W. Helfrich, Appl. Phys. Lett. **18**, 127 (1971).

[2] T. J. Scheffer, and J. Nehring, Appl. Phys. Lett. **45**, 1021 (1984).

[3] S. Matsumoto, M. Kawamoto, and K. Mizunoya, J. Appl. Phys. **47**, 3842 (1976).

[4] P. J. Bos, and K. R. Koehler/Beran, Mol. Cryst. Liq. Cryst. **113**, 329 (1984).

[5] Y. Yamaguchi, T. Miyashita, and T. Uchida, SID Intl. Symp. Digest Tech. Papers **24**, 227 (1993).

[6] K. A. Crandall, M. R. Fisch, R. G. Petschek, and C. Rosenblatt, Appl. Phys. Lett. **65**, 118 (1994).

[7] M. Oh-e, and K. Kondo, Appl. Phys. Lett. **67**, 3895 (1995).

[8] G. D. Boyd, J. Cheng, and P. D. T. Ngo, Appl. Phys. Lett. **36**, 556 (1980).

[9] D. W. Berreman, and W. R. Heffner, Appl. Phys. Lett. **37**, 109 (1980).

[10] W. Greubel, U. Wolf, and H. Kruger, Mol. Cryst. Liq. Cryst. **24**, 103 (1973).

[11] G. P. Bryan-Brown, C. V. Brown, J. C. Jones, E. L. Wood, I. C. Sage, P. Brett, and J. Rudin, SID Intl. Symp. Digest Tech. Papers **28**, 37 (1997).

[12] I. Dozov, M. Nobili, and G. Durand, Appl. Phys. Lett. **70**, 1179 (1997).

[13] J.-X. Guo, Z.-G. Meng, M. Wong, and H.-S. Kwok, Appl. Phys. Lett. **77**, 3716 (2000).

[14] S. H. Lee, K.-H. Park, T.-H. Yoon, J. C. Kim, Appl. Phys. Lett. **82**, 4215 (2003).

[15] S. H. Lee, G.-D. Lee, T.-H. Yoon, and J. C. Kim, Phys. Rev. E **70**, 041704-1 (2004).

[16] C. G. Jhun, J. H. Choi, T.-H. Yoon, and J. C. Kim, Jpn. J. Appl. Phys. **45**, 128 (2006).

[17] S. Saito, T. Takahashi, T. Chiba, and S. Tsuchida, Jpn. J. Appl. Phys. **41**, 3841 (2002).

[18] C. G. Jhun, S. L. Lee, J. H. Choi, T.-H. Yoon, and J. C. Kim, SID Intl. Symp. Digest Tech. Papers **36**, 698 (2005).

[19] C. D. Hoke, and P. J. Bos, J. Appl. Phys. **88**, 2302 (2000).

[20] R. C. Jones, J. Opt. Soc. A. **31**, 488 (1941).

[21] P. Yeh, C. Gu: Optics of liquid crystal displays (A Wiley Interscience Publication, 1999) Chap. 4.

[22] H. S. Kwok, J. Appl. Phys. **80**, 3687 (1996).

[23] S. T. Tang, and H. S. Kwok, J. Appl. Phys. **89**, 5288 (2001).

[24] S. H. Lee, S. H. Hong, J. D. Noh, H. Y. Kim, and D.-S. Seo, Jpn. J. Appl. Phys. **40**, L389 (2001).

[25] C. G. Jhun, C. P. Chen, T.-H. Yoon, and J. C. Kim, Jpn. J. Appl. Phys. **45**, 5117 (2006).

[26] B. Bahadur: Liquid Crystals applications and uses (Word Scientific Publishing Co. Pte. Ltd., 1990) Chap. 8.